NANO · MICRO small

Supporting Information

for *Small*, DOI 10.1002/smll.202308610

Platinum-Grafted Twenty-Five Atom Gold Nanoclusters for Robust Hydrogen Evolution

Paloli Mymoona, Jose V. Rival, Nonappa, Edakkattuparambil Sidharth Shibu and Chinnaiah Jeyabharathi**

Supporting Information

Platinum-Grafted Twenty-Five Atom Gold Nanoclusters for Robust Hydrogen Evolution

Paloli Mymoona, Jose V. Rival, Nonappa, Edakkattuparambil Sidharth Shibu, Chinnaiah Jeyabharathi**

S1: ECSA calculation

The ECSA can be evaluated using the following equation.

$$\mathrm{ECSA} = \frac{Q_\mathrm{C}}{Q_\mathrm{S}}$$

Where Q_C is the charge associated with the normalized area from the cyclic voltammogram and Q_S is the charge corresponding to, gold oxide reduction (390 μC cm^{-2}), deposition of monolayer Pb on gold (300 μC cm^{-2}), and monolayer coverage of H atoms onto polycrystalline Pt (210 μC cm^{-2}) respectively.

S2: ECSA calculation of Pt-Au_{25} NCs

The ECSA of Pt-Au_{25} NCs determined from CV with various negative potentials, yielding values of 0.0371, 0.0151, 0.0145, 0.0057, and 0.0006 cm^2, corresponding to limiting potentials of -0.25, -0.24, -0.23, -0.22, and -0.21 V, respectively. ECSA becomes steady with the vertex potential of -0.24 and -0.23 V (inset of **Figure S3**a). Thus, we chose -0.23 V to evaluate the ECSA value as it might include less contribution from hydrogen oxidation (**Figure S3**b). With this ECSA value, the overpotential for Pt-Au_{25} NCs shifts from 0.164 V *vs* RHE to 0.117 V *vs* RHE when considering an ECSA from 0.0371 to 0.0145 cm^2 (**Figure S3**b)

S3: Calculation of the amount of Pt in Pt-Au_{25} NCs

To determine the Pt content in Pt-Au_{25} NCs prepared *via* the electroless grafting method, we employed a calculation based on the charge associated with hydrogen desorption (**Figure S3**a). This calculation assumes that all Pt atoms are exposed since the decoration is limited to the surface and takes into account the single electron transfer as described by the equation, $\mathrm{Pt-H} \rightarrow \mathrm{Pt} + \mathrm{H}^+ + e^-$. The loading of Pt achieved through the electroless decoration process was determined to be 0.8 μg cm^{-2} from the hydrogen stripping charge (30.45 μC). It's worth noting that this loading is 7 times lower when compared to the Pt/C (5.7 μg cm^{-2} of Pt).

S4: Optimization of electrochemical activation

The influence of activation time on HER activity of EC-Au_{25} NCs was conducted by changing the activation time 2, 4, 6, 8, and 10 s of the Au_{25} NCs on a GCE. **Figure S8** shows the polarization curves of EC-Au_{25} NCs in 0.1 M H_2SO_4 between the potentials of 0.2 to -0.8 V RHE at 5 mV s^{-1}. The HER activity increases up to 6 s and after 6 s the reactivity starts declining. Hence, we opted for 1 s as a suitable treatment time for not to damage the cluster integrity.

S5: Optimization of immersion time in chloroplatinic acid

The effect of immersion time in chloroplatinic acid on the Pt loading was studied by utilizing various immersion times, namely, 5, 10, and 15 minutes in a chloroplatinic acid solution. **Figure S9** shows the polarization curves of Pt-Au_{25} NCs in 0.1 M H_2SO_4 between the potentials of 0.2 to -0.6 V *vs* RHE at 5 mV s^{-1}. The HER activity of these Pt-Au_{25} NCs, as evidenced by their onset potential, remained unchanged. This suggests that the quantity of Pt atoms decorated on the surface of EC-Au_{25} NCs is limited by adsorbed hydrogen on gold, which is a kind of self-termination process and thus not dependent on the immersion time in chloroplatinic acid.

S6: Effect of the counter electrode on HER activity

To ensure that the dissolution of the Pt from the counter electrode does not impact the reactivity of the NCs at the working electrode where the dissoluted Pt can be redeposited, we conducted a control experiment with both Pt and graphite counter electrodes. The HER activity of EC-Au_{25} and Pt-Au_{25} NCs was then compared by using two different counter electrodes such as Pt wire and graphite rod against Ag/AgCl as a reference electrode with a potential window of 0.2 to -0.8 V with a scan rate of 5 mV s^{-1} as shown in **Figure S10**. The overpotential corresponding to 10 mA cm^{-2} *vs* RHE of EC-Au_{25} and Pt-Au_{25} NCs corresponding to both Pt wire and graphite rod is comparable to one another, implying that the Pt is not dissoluted from the Pt counter electrode. Since there was no change in the catalytic activities, the possibility of Pt leaching is ruled out. This is also understandable from the fact that the surface area ratio between the Pt counter electrode and the working electrode is *ca*. 28.5.

S7: Effect of the working electrode on HER activity

The HER activity of EC-Au_{25} and Pt-Au_{25} NCs was further compared by using GC disk and plate (1×1 cm^2) working electrodes (**Figure S11**). The overpotential corresponding to 10 mA

cm^{-2} *vs* RHE of EC-Au_{25} and Pt-Au_{25} NCs corresponding to both working electrodes is comparable to one another showing the reliability of experiments.

S8: Effect of concentration of electrolyte on HER activity

The effect of the concentration of electrolytes (**Figure S12**a and b) on the HER performance of EC-Au_{25} and Pt-Au_{25} NCs was studied. The effect of the concentration of electrolyte was studied by taking different concentrations of H_2SO_4 from 20-100 mM and recorded LSV at potentials between 0.2 to -0.8 V *vs* Ag/AgCl and 0.2 to -0.4 V *vs* Ag/AgCl at 5 mV s^{-1} for EC-Au_{25}, and Pt-Au_{25} NCs respectively. The study showed that while increasing the concentration of electrolytes from 20-100 mM, the current density is increased and the overpotential positively shifted in the case of both catalysts, as shown in **Figure S12**a and b. The current density enhancement while increasing the concentration of the sulfuric acid points to the enhanced flux of protons.

S9: Effect of catalyst loading on HER activity

The influence of catalytic loading on HER activity was conducted by coating 2, 4, 6, 8, and 10 µL of the Au_{25} NCs on a GCE. **Figure S13**a and b shows the polarization curves of EC-Au_{25} and Pt-Au_{25} NCs in 0.1 M H_2SO_4 between the potentials of 0.2 to -0.4 V *vs* RHE at 5 mV s^{-1}. In the case of both catalysts, the current density is increased as well and the overpotential is shifted positively is attributed to the higher loading of the catalyst leading to exposure to more active sites after EC-activation, and also more Pt atoms are assumed to be fabricated. The impact of increasing ECAS while increasing the loading of NCs can be witnessed with the positive shift in the overpotentials.

S10: Calculation of elemental composition from XPS

The elemental composition from Au_{25}, EC-Au_{25}, and Pt-Au_{25} NCs was evaluated by comparing the atomic percentage ratios of Au, S, and Pt using the corresponding XPS data. This analysis involved assessing the normalized area of the XPS deconvoluted peaks. Normalization was performed using respective relative sensitivity factors (RSF) for the specific elements and electronic states (**Table S2**).

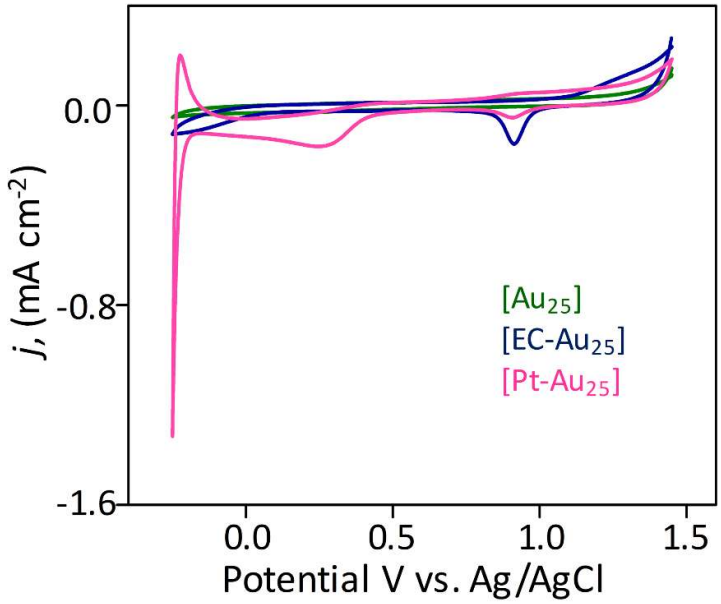

Figure S1. Cyclic voltammogram of Au_{25}, EC-Au_{25}, and Pt-Au_{25} NCs in O_2-saturated 0.1 M H_2SO_4 at 50 mV s^{-1} from -0.2 to 1.45 V vs. Ag/AgCl

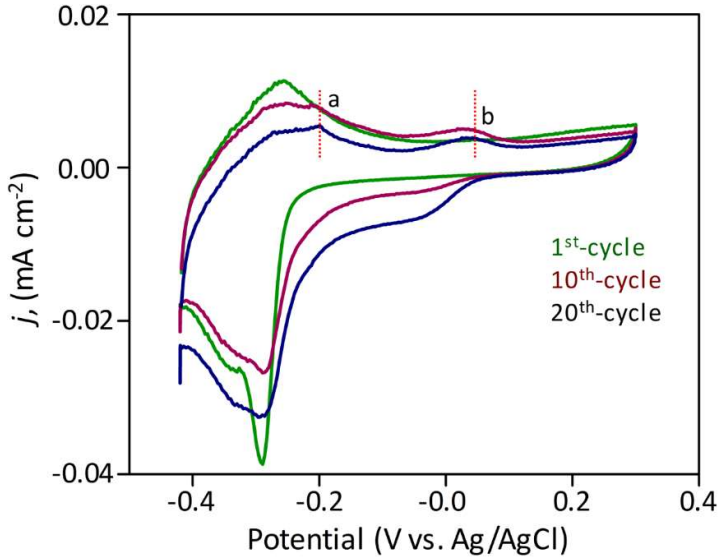

Figure S2. Cyclic voltammogram of EC-Au_{25} NCs from the 1st to 20th cycles of Pb-UPD from -0.4 to 0.3 V vs. Ag/AgCl at 20 mV s^{-1}. "a" and "b" corresponds to Au(111) and Au (110), respectively.

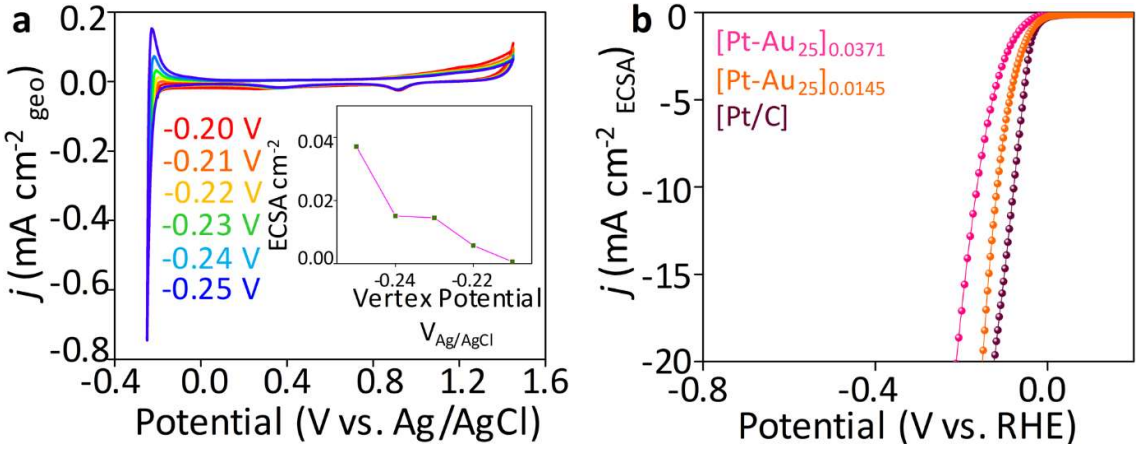

Figure S3. (a)The CV of Pt-Au_{25} NCs in 0.1 M H_2SO_4 at different vertex potentials 100 mV s^{-1}. The plot of vertex potentials vs ECSA in the inset. (b) HER polarization curves of Pt-Au_{25} NCs (normalized with ECSA 0.0371 and 0.0145 cm^2) and Pt/C in 0.1 M H_2SO_4 at 5 mV s^{-1}.

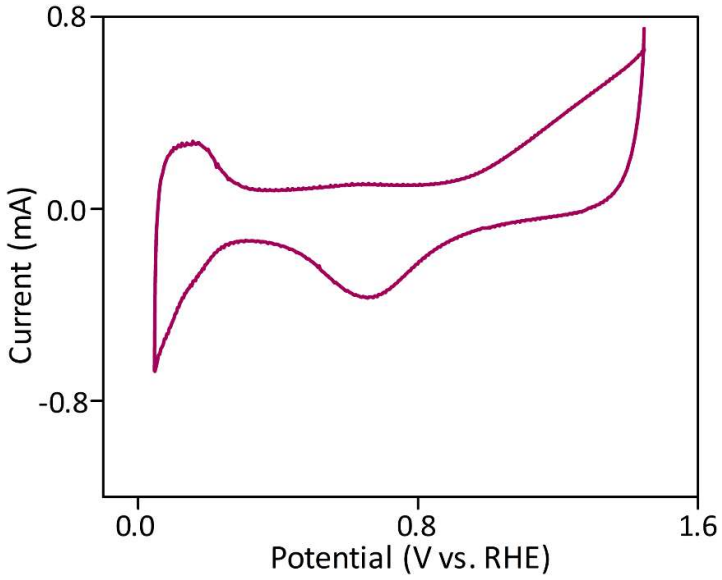

Figure S4. Cyclic voltammogram of Pt/C catalyst in N_2 mediated 0.1 M H_2SO_4 at 100 mV s^{-1} from 0 to 1.45 V vs. RHE.

.

a Sample Concentration (ng/mL)	Component RT	Peak Area
PET 500	6.8696	11457.2
PET 1000	6.8697	23167.9
PET 1500	6.8698	32195.5
PET 2000	6.8696	46538.7
Sample without standard	6.8754	27259.8
Sample with PET 1000	6.8697	51207.3

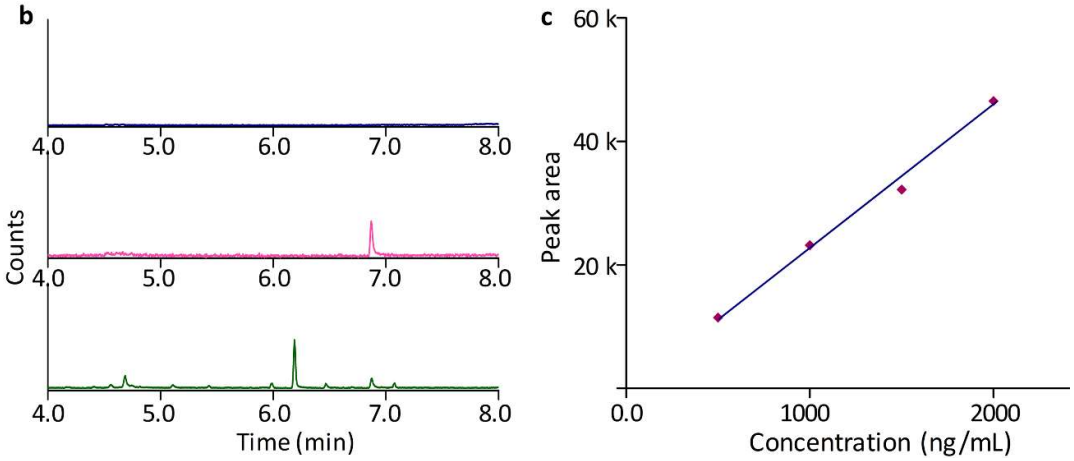

Figure S5. (a) Summarized GC-MS data of removed PET. (b) GC-MS chromatogram shows the separation and retention time of acetonitrile, standard PET solution with 1000 ng mL^{-1}, and sample PET. (c) Calibration curves of PET standard solutions having concentrations 500, 1000, 1500, and 2000 ng mL^{-1}.

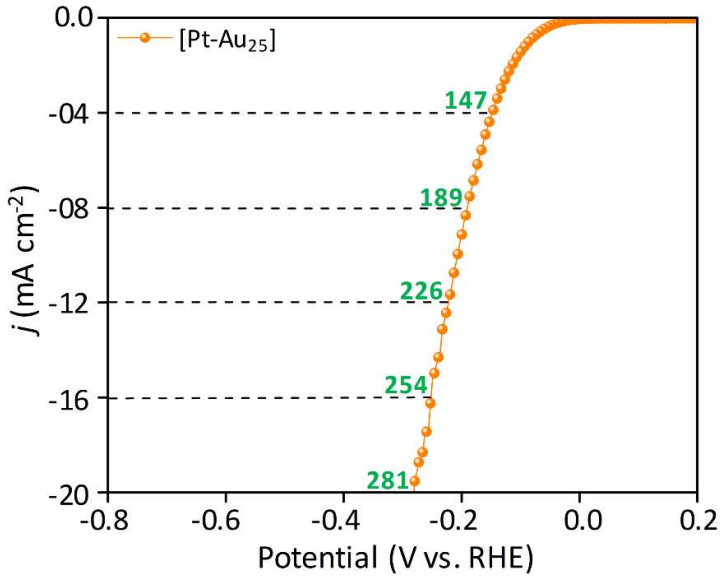

Figure S6. HER polarization curve of the Pt-Au_{25} NCs. in N_2 mediated 0.1 M H_2SO_4 showing the milliampere level current densities.

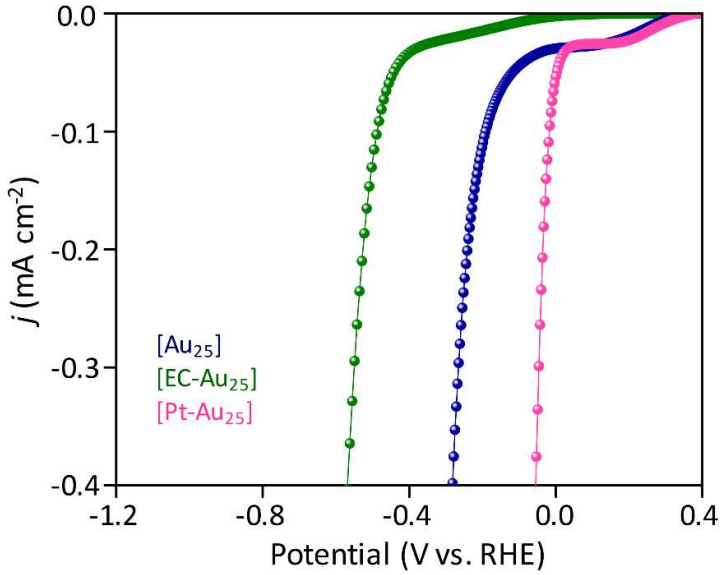

Figure S7. The polarization curve of Au_{25}, EC-Au_{25}, and Pt-Au_{25} NCs in 0.1 M H_2SO_4 at 5 mV s^{-1} from 0.2 to -1.2 V vs. RHE shows the enlarged graphs in the low-potential region.

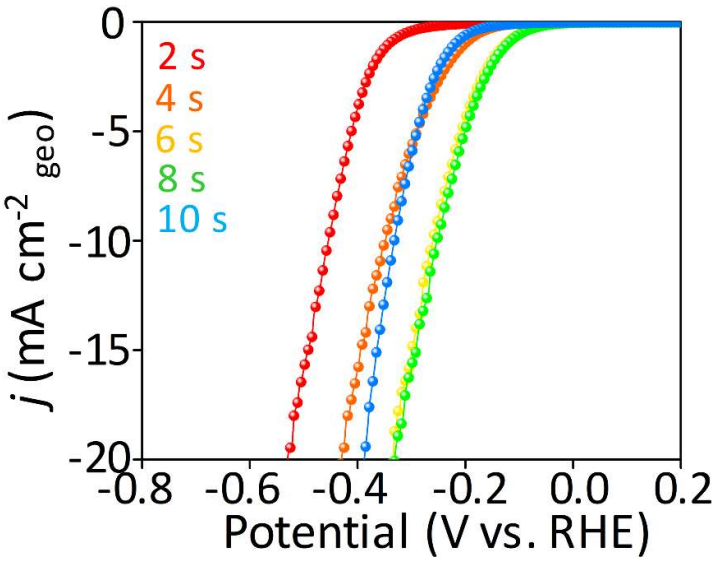

Figure S8. HER polarization curves of EC-Au_{25} NCs in different activation times in 0.1 M H_2SO_4 at 5 mV s^{-1} from 0.2 to -0.8 V vs. RHE.

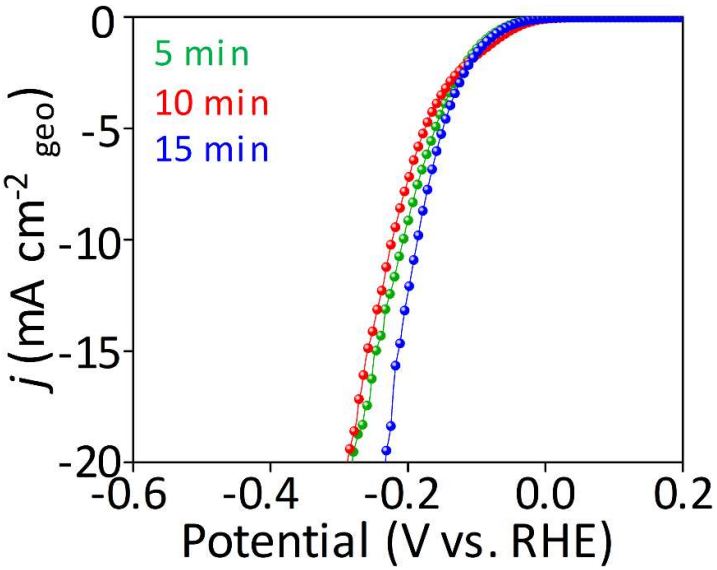

Figure S9. HER polarization curves of Pt-Au_{25} NCs with different immersion time of EC-Au_{25} NCs in chloroplatinic acid in 0.1 M H_2SO_4 at 5 mV s^{-1} from 0.2 to -0.8 V vs. RHE.

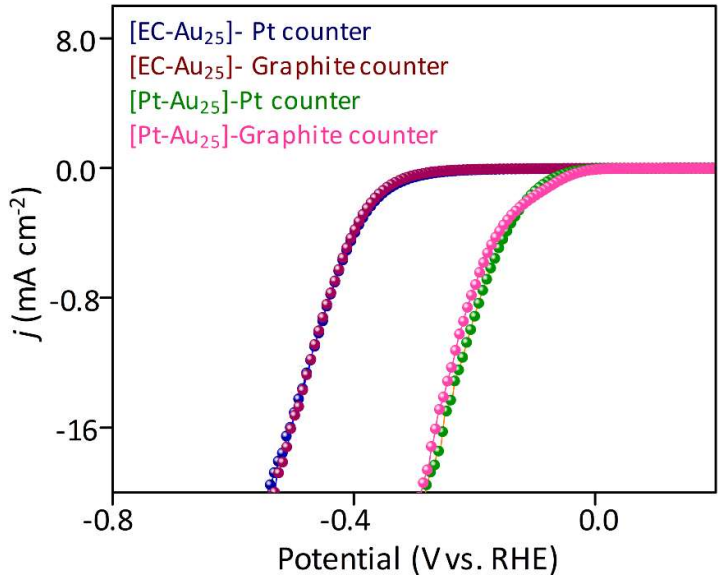

Figure S10. Polarization curve of EC-Au_{25} and Pt-Au_{25} NCs using Pt wire and graphite rod as counter electrodes in 0.1 M H_2SO_4 at 5 mV s^{-1} from 0.2 to -0.8 V vs. RHE.

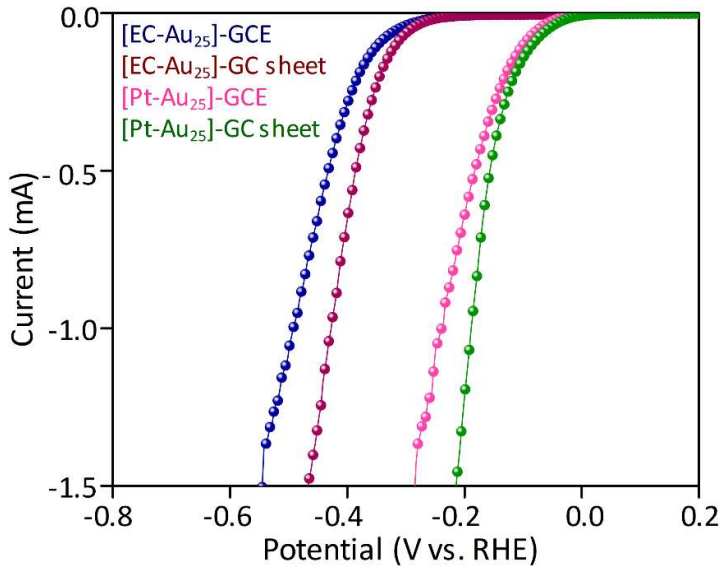

Figure S11. Polarization curve of the EC-Au_{25} and Pt-Au_{25} NCs using glassy carbon electrode (GCE) and glassy carbon plate (1×1 cm^2) electrode as working electrodes in 0.1 M H_2SO_4 at 5 mV s^{-1} from 0.2 to -0.8 V vs. RHE.

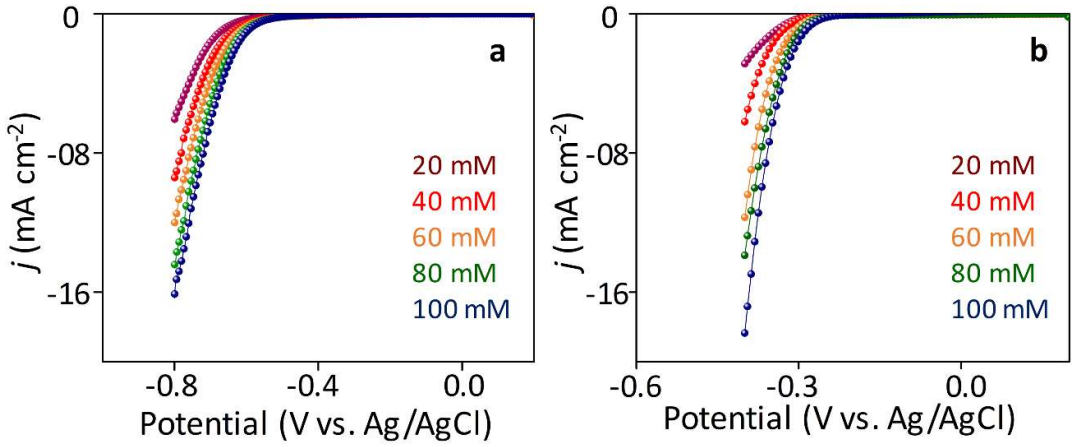

Figure S12. Polarization curves of (a) EC-Au_{25} and (b) Pt-Au_{25} NCs in different concentrations of H_2SO_4 at 5 mV s^{-1} from 0.2 to -0.8 V vs. Ag/AgCl and 0.2 to -0.4 V vs. Ag/AgCl respectively.

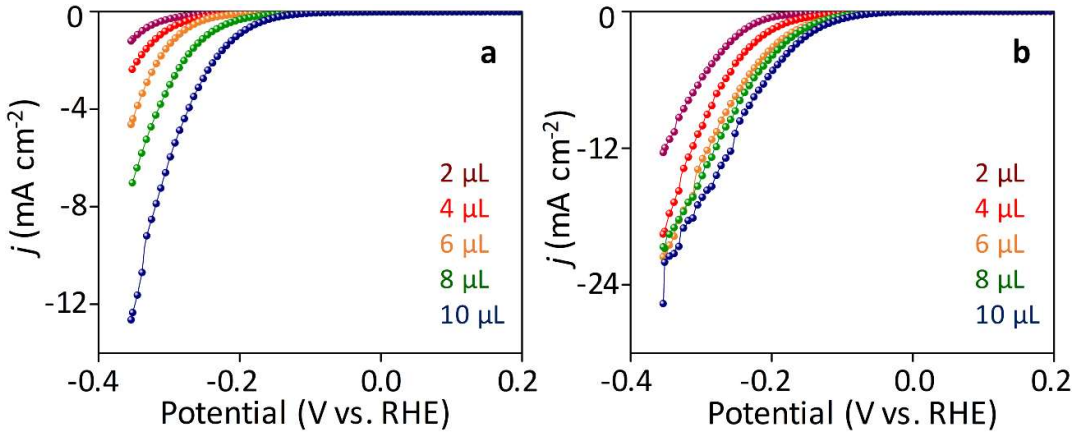

Figure S13. Polarization curves of (a) EC-Au_{25} and (b) Pt-Au_{25} NCs in different catalytic loading in 0.1 M H_2SO_4 at 5 mV s^{-1} from 0.2 to -0.4 V vs. RHE respectively.

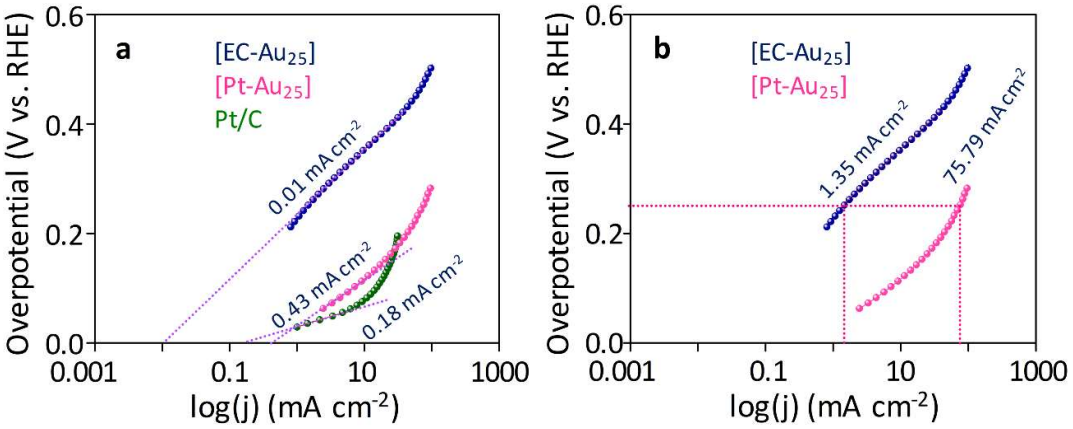

Figure S14. (a) Extrapolation of Tafel slope to zero overpotentials for the calculation of exchange current density (j_0) of EC-Au_{25}, Pt-Au_{25}, and Pt/C. (b) Specific activity of EC-Au_{25} and Pt-Au_{25} at an overpotential of 0.25 V.

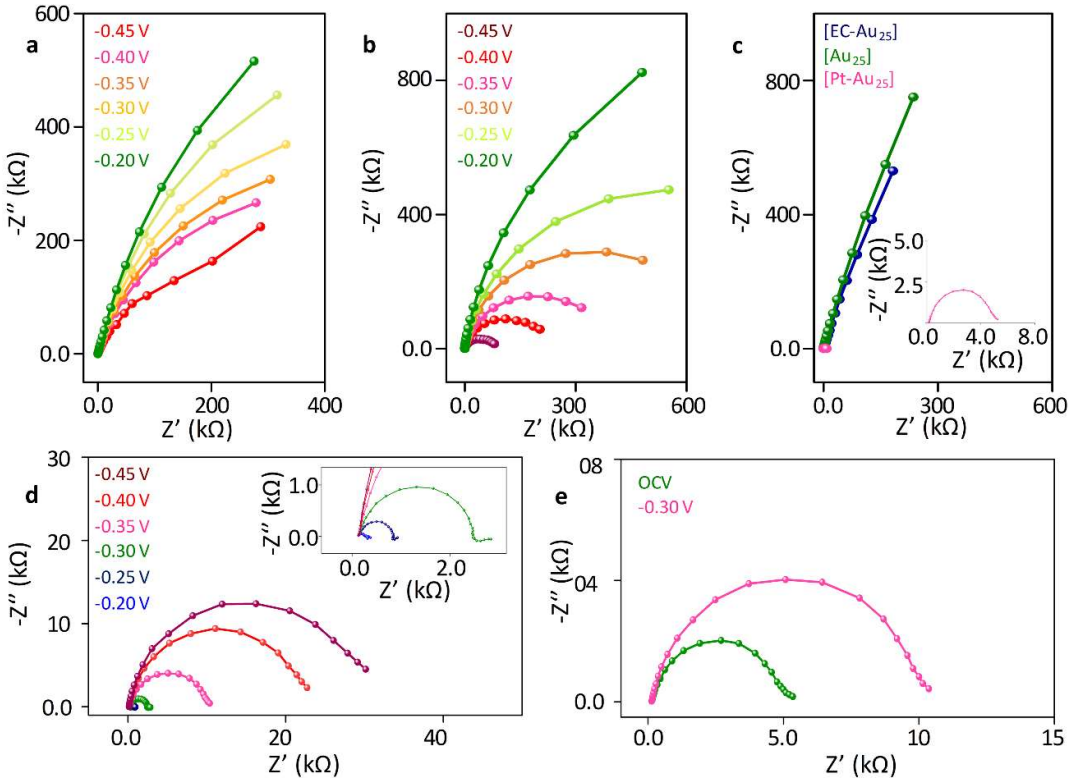

Figure S15. Nyquist plot of (a) Au_{25} NCs, (b) EC-Au_{25} NCs, and (d) Pt-Au_{25} NCs (EIS of higher potentials are shown in the inset of Figure. 13d) at different overpotentials (c) Nyquist plot of Au_{25} NCs, EC-Au_{25} NCs, and Pt-Au_{25} NCs at OCV. The zoom-in EIS of Pt-Au_{25} is shown in the inset. (e) Nyquist plot of Pt-Au_{25} NCs at OCV and 300 mV.

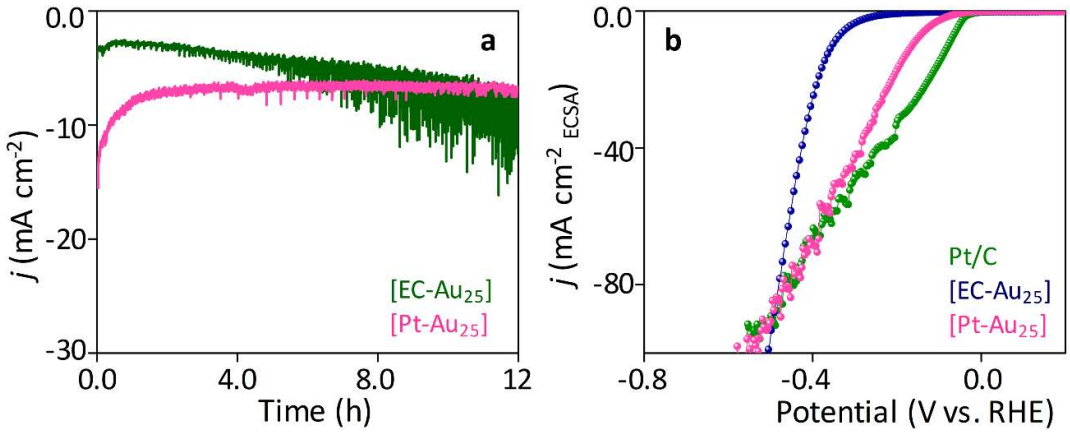

Figure S16. (a) Chronoamperometry plots of EC-Au_{25} and Pt-Au_{25} NCs at a constant potential to achieve an initial current density of 10 mA cm^{-2}. (b) The HER polarization curve of Pt/C, EC-Au_{25}, and Pt-Au_{25} NCs in 0.1 M H_2SO_4 at 5 mV s^{-1} from 0.2 to -1.2 V vs. RHE shows the higher current density region.

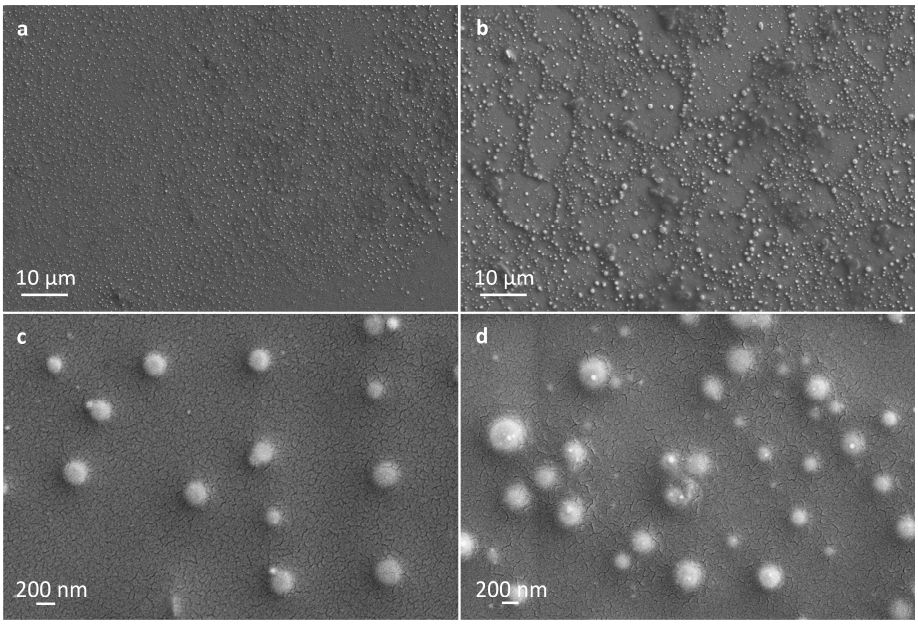

Figure S17. FE-SEM of (a,c) EC-Au_{25} and (b,d) Pt-Au_{25} NCs

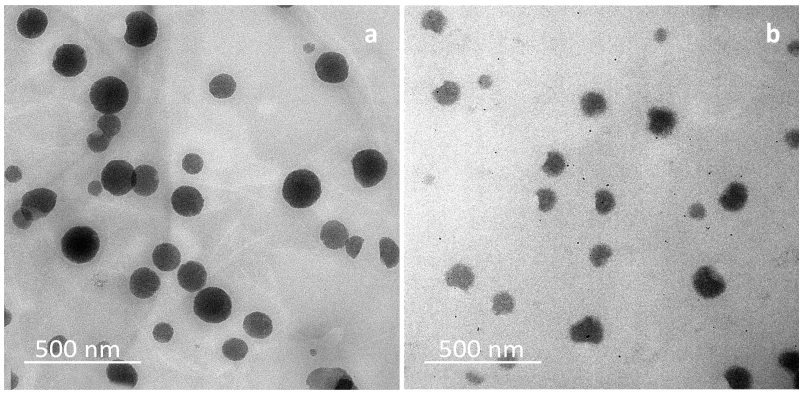

Figure S18. Large area TEM images of the (a) EC-Au_{25}, and (b) Pt-Au_{25} NCs.

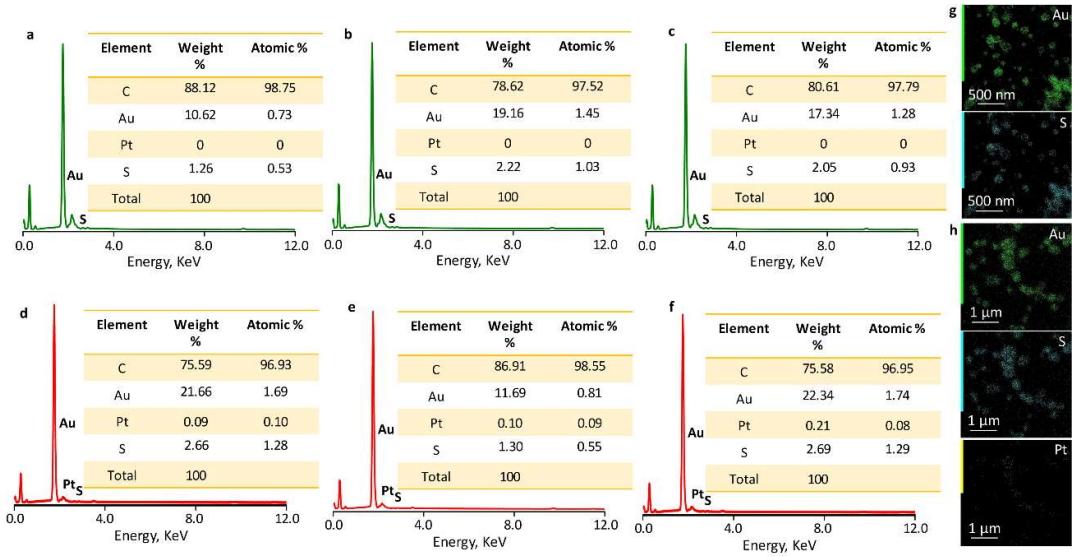

Figure S19. EDS analysis of (a-c) EC-Au_{25} and (d-f) Pt-Au_{25} NCs. Corresponding elemental compositions are shown in the inset HAADF-STEM images of the EC-Au_{25} NC. Elemental mapping of the (g) EC-Au_{25} (Au and S) and (h) Pt-Au_{25} NCs (Au, S, and Pt), respectively.

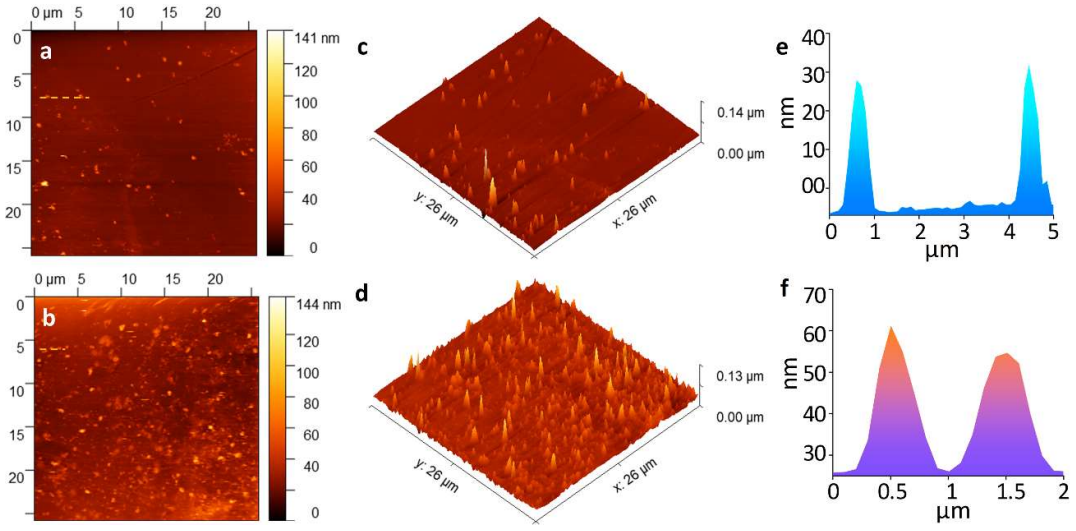

Figure S20. AFM images (a,b) topography (c,d) amplitude and corresponding (e,f) height profile of EC-Au_{25}, and Pt-Au_{25} NCs.

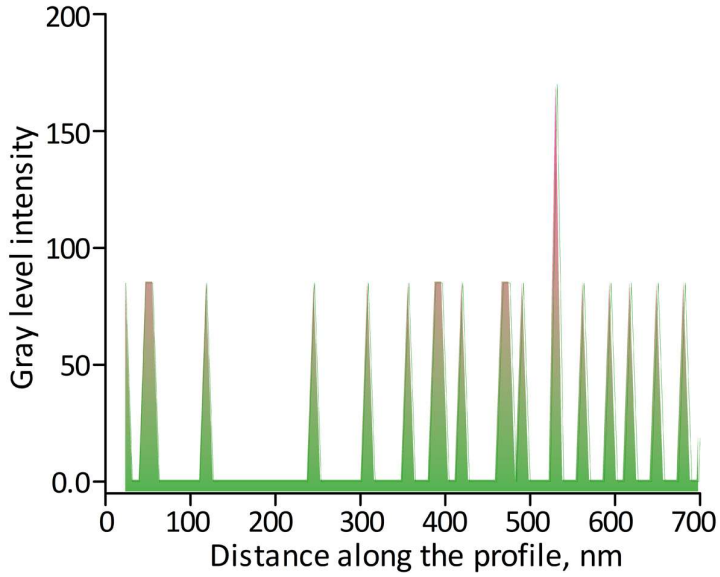

Figure S21. Gray level intensity profile of Pt-atoms in Pt-Au_{25} NCs.

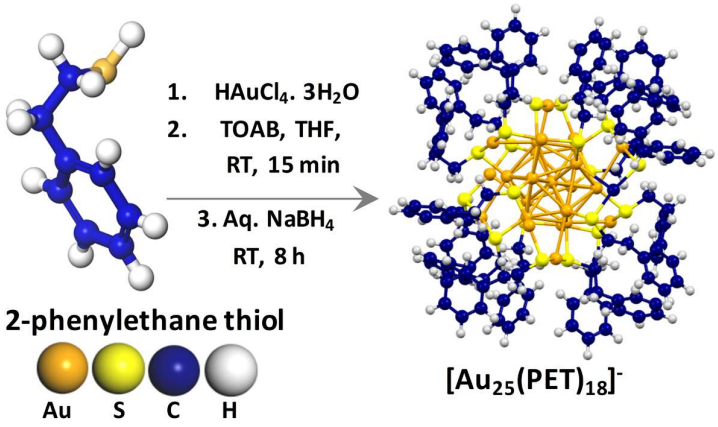

Scheme S1: Schematic representation of the synthesis of Au_{25} NCs.

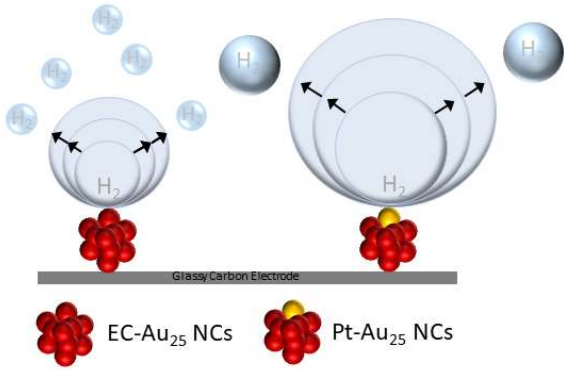

Scheme S2: Schematic representation of bubble formation on the surface of EC-Au_{25} and Pt-Au_{25} NCs.

Catalyst	Method	Charge (Qc, μC)	Charge (Qs, μC cm^{-2})	ECSA (cm^2)
Pt/C	CV in 0.1 M H_2SO_4	36.7	210	0.1747
EC-Au_{25}	CV in 0.1 M H_2SO_4	4.408	390	0.0113
EC-Au_{25}	Pb-UPD	3.423	300	0.0114
Pt-Au_{25}	CV in 0.1 M H_2SO_4	30.45	210	0.0145

Table S1: Calculation of ECSA of EC-Au_{25}, and Pt-Au_{25} NCs.

Sample	Element	Peak Area	RSF	Corrected Area[a]	Atomic Percentage
Au_{25} NCs	Au	45768.48	17.12	2673.04	53.15
	S	3957.38	1.68	2355.58	46.84
EC-Au_{25} NCs	Au	29358.76	17.12	1714.14	60.41
	S	1123.77	1.68	1123.77	39.58
Pt-Au_{25} NCs	Au	19939.25	17.12	1164.67	46.17
	S	1510.19	1.68	898.92	35.63
	Pt	7094.52	15.46	458.89	18.18

[a] All areas are corrected for the relative sensitivity factor (RSF), the transmission factor (T), and the mean free path (MFP).

Table S2: Calculation of atomic composition of Au_{25}, EC-Au_{25}, and Pt-Au_{25} NCs from XPS data.